



OPEN

# Photoresponsive Supramolecular Complexes as Efficient DNA Regulator

SUBJECT AREAS:

SELF-ASSEMBLY

MOLECULAR MACHINES AND  
MOTORS

Hong-Bo Cheng, Ying-Ming Zhang, Chao Xu &amp; Yu Liu

Department of Chemistry, State Key Laboratory of Elemento-Organic Chemistry, Nankai University, Collaborative Innovation Center of Chemical Science and Engineering, Tianjin 300071, P. R. China.

Received

27 September 2013

Accepted

11 February 2014

Published

27 February 2014

Correspondence and  
requests for materials  
should be addressed to  
Y.L. (yuliu@nankai.  
edu.cn)

Two supramolecular complexes of *trans*-1 $\subset$ CB[8] and *trans*-2 $\subset$ CB[8] were successfully achieved by the controlled selective complexation process of cucurbit[8]uril (CB[8]) with hetero-guest pair containing azobenzene and bispyridinium moieties in aqueous solution, exhibiting the reversibly light-driven movements of CB[8] upon the photocontrollable isomerization of azophenyl axle components. Significantly, the obtained bistable supramolecular complexes and their corresponding [2]pseudorotaxanes could act as a promising concentrator and cleavage agent to regulate the binding behaviors with DNA molecules.

Artificial molecular machines, originated from the integrative self-assemblies of intermolecular components to act as machine-like motions in response to external stimuli, have attracted an upsurge of attention in the progressive miniaturization of electronic devices<sup>1–4</sup>. Consequently, considerable endeavors have been devoted to exploring and mimicking the realistic prototype in the macroscopic world, and a great number of artificial molecular machines with shuttling, rotation, and threading/dethreading motions, including molecular brake<sup>5</sup>, molecular gyroscope<sup>6</sup>, molecular elevator<sup>7</sup>, molecular scissors<sup>8</sup>, and dual-modulated molecular switch<sup>9</sup>, have been elaborately designed and synthesized over the past decades. For instance, Kim et al. have made the pioneering contributions to the construction of cucurbituril-mediated molecular loop locks, in which the electrochemically triggered interconversion could be reversibly controlled between the folding of radical cation dimers and unfolding of pseudorotaxane structures<sup>10,11</sup>. Moreover, using the light-responsive isomerization of azobenzene, Scherman et al. have reported a photoirradiation method to control over the stoichiometry of cucurbituril-containing inclusion complexes, ultimately implementing a host-guest polymeric system in both solution and the solid state<sup>12</sup>.

The construction of molecular machines has attracted increasing attention in different fields<sup>12,13</sup>. However, modulating the morphology and function of biomacromolecules by using the reversible residence of macrocyclic hosts with unique trigger mode, remains challenging<sup>14–16</sup>. Within this regard, we have previously constructed a reversible 2D cationic polypseudorotaxane under acidic and basic conditions, thus exhibiting a controlled DNA regulator by varying the amount of cucurbit[6]urils (CB[6]) on the pendant substituents<sup>17,18</sup>. These findings prompt us to hypothesize that the modulation of mechanical motions and their biological functions may be simplified by properly utilizing light and thermal stimuli in these bioactive switching systems, because the switching process involving light- and thermo-driven complexes always occurs in a rapid and precise way with high sensitivity and fast response duration<sup>19–21</sup>. Although the inclusion complexation behaviors of CB[8] with positively charged azobenzene was reported<sup>13</sup>, our major interest herein is to develop the biological application of the CB-based supramolecular complexes.

To verify the hypothesis, in the present work, we report two supramolecular complexes arising from the noncovalent interactions of CB[8] with azobenzene and bispyridinium salts, in which the capture and releasing of bispyridinium guests could be reversibly manipulated using light and thermal energy as external inputs. Different from the doubly charged reference axle linked by alkyl chains, the unconventional movement of CB[8] on the triply charged axle molecule was ascribable to the imidazolium unit that can efficiently adjust the binding mode of CB[8] with azophenyl *cis*-isomer and then keep CB[8] docking at the end of azobenzene. More significantly, it is found that the resultant supramolecular complexes and [2]pseudorotaxanes could be considered as an efficient regulator in controlling the condensation and photocleavage behaviors of DNA, which can energize the practical use of molecular machines in biological field, as illustrated in Figure 1.

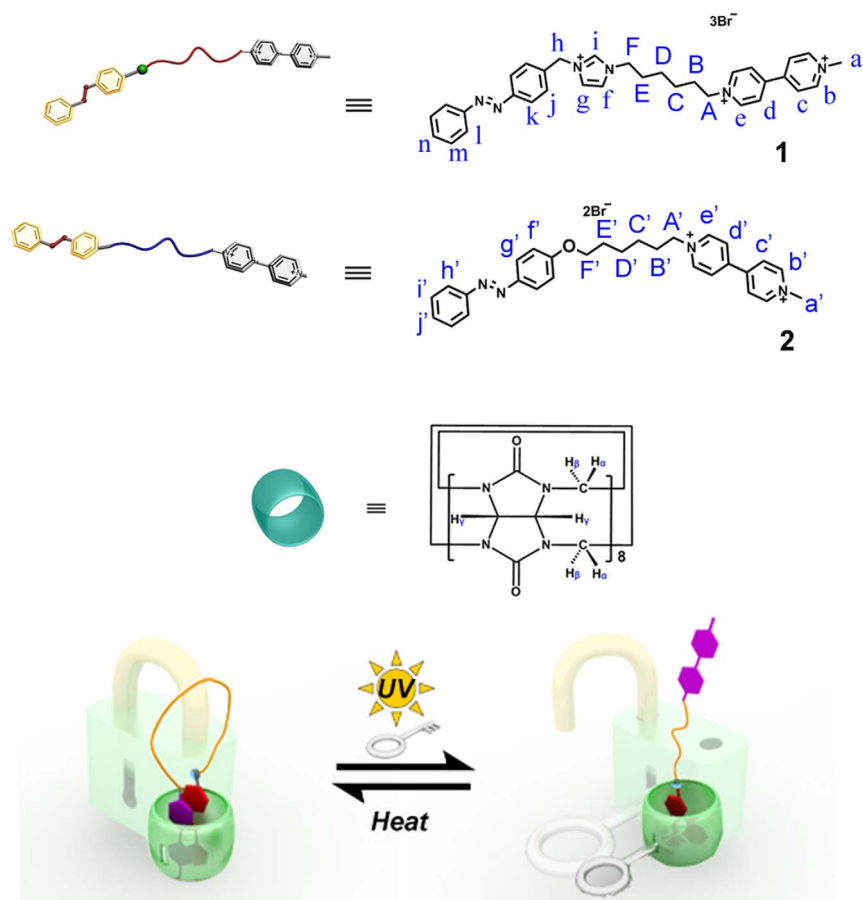


**Figure 1** | Molecular Structures of **1**, **2**, CB[8], and Schematic Representation of Controlled Interconversion Process between the Supramolecular Complexes and [2]Pseudorotaxane.

## Results

**Synthesis of axles 1, 2 and 3.** The triply charged acceptor–donor–type linear molecule (**1**) was synthesized by the reaction of (*E*)-1-(4-(phenyldiazenyl)benzyl)-1*H*-imidazole with 1-(6-bromohexyl)-1'-methyl-4,4'-bipyridine-1,1'-dium bromide iodide, followed by the protonation and the counterion exchange (Supplementary Figure S1). Meanwhile, the doubly charged axle molecule (**2**) without imidazolium group was also obtained in a similar procedure. Furthermore, in order to clearly demonstrate the individual roles of bispyridinium and azophenyl moieties, two compounds of methyl viologen ( $MV^{2+}$ ) and 4-(*N*-ethylimidazol)-azobenzene (**3**) were synthesized as references. The characteristic  $^1H$  resonances in compound **1** and **2** were clearly assigned by the use of 2D NMR correlation spectroscopy (COSY) recorded in  $D_2O$  (Supplementary Figures S14 and S15).

**The binding stability of complex  $trans\text{-}3 \cdot MV^{2+} \subset CB[8]$  was validated by ITC experiment.** In this case, the binding affinity of inclusion complex  $trans\text{-}3 \cdot MV^{2+} \subset CB[8]$  was measured by the isothermal titration calorimetry (ITC) experiment, giving the binding stability constant ( $K_S$ ) up to  $10^9 M^{-2}$  for this ternary complex (Supplementary Figures S16 and S17). This result indicates the high affinity of CB[8] toward the positively charged azobenzene and bispyridinium unit, which can facilitate the eventual formation of bistable supramolecular complexes of  $1 \subset CB[8]$  and  $2 \subset CB[8]$  as described below.

**The controlled interconversion process between the supramolecular complexes  $trans\text{-}1 \subset CB[8]$  and [2]pseudorotaxane  $cis\text{-}1 \subset CB[8]$  were investigated by  $^1H$  NMR titration experiments.**

Based on the aforementioned results of  $trans\text{-}3 \cdot MV^{2+} \subset CB[8]$  system, the binding process between the guest molecule *trans*-**1** and CB[8] can be conveniently monitored by  $^1H$  NMR spectroscopy. As discerned from Figure 2a and 2b, the proton signals of  $H_{b-e}$  in bispyridinium moiety and  $H_{k,m,n}$  in *trans*-azobenzene moiety of **1** gave obvious upfield shifts, whereas the ones of  $H_g$  in the imidazolium ring and  $H_{B-F}$  in the alkyl linkers showed a notable downfield shift in the presence of 1.0 equiv of CB[8]. Therefore, it can be concluded that the bispyridinium and *trans*-azobenzene units of *trans*-**1** were concurrently encapsulated in the cavity of CB[8] with pendant alkyl linkers outside the cavity.

Moreover, benefiting from the slow exchange equilibrium, both free and bound guest molecules (defined as *trans*-**1**<sub>free</sub> and *trans*-**1**<sub>bound</sub>) could be distinguishable on the  $^1H$  NMR time scale (Supplementary Figure S18). Then,  $^1H$  NMR titration experiments were carried out to investigate the complex stoichiometry between *trans*-**1** and CB[8]. As shown in Supplementary Figure S19, the ratio curve of  $[trans\text{-}1_{free}]/[trans\text{-}1_{bound}]$  versus  $[CB[8]]/[trans\text{-}1]$  showed an inflection point at 1.0 to determine the formation of 1 : 1 host–guest complex, which was further supported by Job's plot (Supplementary Figure S20). Moreover, combined the results of 2D NMR analyses, it is suggested that the aromatic units of bispyridinium and azobenzene parts were encapsulated in the cavity of CB[8] to form the supramolecular complex *trans*-**1**⊂CB[8] (Supplementary Figures S21 and S22). Furthermore, an excess amount of CB[8] and  $\alpha$ -cyclodextrin ( $\alpha$ -CD) was added to examine the stability of supramolecular complex (Supplementary Figures S23), and no obvious change in the chemical shifts or peak patterns was observed, indicative of the high stability and affinity of this obtained supramolecular complex.

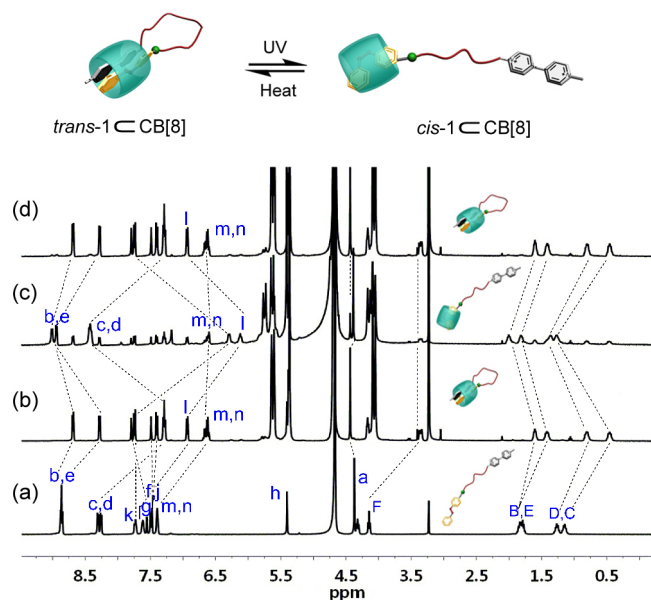


**Figure 2** |  $^1\text{H}$  NMR titration experiments of axle 1 and CB[8] (400 MHz,  $\text{D}_2\text{O}$ ). (a) *trans*-1; (b) *trans*-1 $\subset$ CB[8]; (c) *trans*-1 $\subset$ CB[8] after sufficient photoirradiation at 365 nm; (d) the corresponding solution in (c) after standing in the dark at  $80^\circ\text{C}$  for 12 h ( $[\textit{trans}\text{-}1] = [\text{CB}[8]] = 1.0 \text{ mM}$ ).

In addition, the formation of supramolecular complex *trans*-1 $\subset$ CB[8] was further confirmed by mass spectrometry. The corresponding peaks at  $m/z$  616.4 and 964.0 were assigned to  $\{\textit{trans}\text{-}1\subset\text{CB}[8] - 3\text{Br}\}^{3+}$  and  $\{\textit{trans}\text{-}1\subset\text{CB}[8] - 2\text{Br}\}^{2+}$ , respectively (Supplementary Figure S30). Moreover, the molecular energy minimization was also carried out to confirm the proposed loop structure, in which two aromatic guests were in close proximity around the portal of CB[8] (Supplementary Figure S34). Combining all of these results, we can reasonably deduce the formation of the supramolecular complex *trans*-1 $\subset$ CB[8].

It is well-documented that the photochemical process involving photochromic azobenzene derivatives could be reversibly controlled, due to their unique properties of photoinduced *trans*- and *cis*-isomerization under UV and visible light.  $^1\text{H}$  NMR characterization was further conducted to confirm the controlled interconversion process from supramolecular complex *trans*-1 $\subset$ CB[8] to [2]pseudorotaxane *cis*-1 $\subset$ CB[8]. As shown in Supplementary Figure S26, the axle molecular *trans*-1 was accordingly transferred to *cis*-1 under irradiation at 365 nm with the ratio of 28:72 between *trans*- and *cis*-forms. When the equimolar mixture of *trans*-1 and CB[8] was irradiated by UV light, the proton signals of  $\text{H}_{\text{b-e}}$  in bispyridinium moiety and  $\text{H}_{\text{B-E}}$  in the alkyl linkers of 1 underwent an obvious downfield shift, whereas the characteristic peaks of protons  $\text{H}_{\text{k,l}}$  in electron-rich azobenzene of *cis*-1 shifted to higher field (Figure 2c). These phenomena jointly indicate that the azobenzene group of the *cis*-1 was still bound in the cavity of CB[8], whereas the rest of guest *cis*-1 was released from the cavity to form [2]pseudorotaxane *cis*-1 $\subset$ CB[8]. Similarly, the loop structure of *trans*-1 $\subset$ CB[8] could be recovered to the original state upon heating treatment, due to the *cis*- and *trans*-thermoisomerization of 1 (Figure 2d). Moreover, the results of diffusion ordered spectroscopy (DOSY) experiments<sup>22–24</sup> could reasonably exclude the possibility of 2:2 complex or  $n:n$  formation of polymeric species and further confirm the interconversion of two major supramolecular species (supramolecular complex *trans*-1 $\subset$ CB[8] and [2]pseudorotaxane *cis*-1 $\subset$ CB[8]) by UV irradiation (Supplementary Figures S24 and S25).

#### The controlled interconversion process between the supramolecular complex *trans*-1 $\subset$ CB[8] and [2]pseudorotaxane *cis*-1 $\subset$ CB[8]

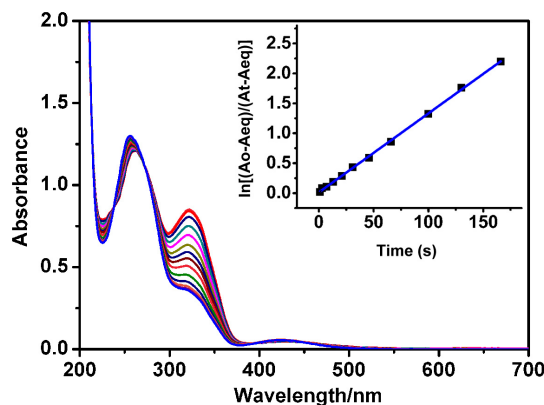


**Figure 3** | UV/vis spectroscopic titration of *trans*-1 $\subset$ CB[8] (0.1 mM) to determine the photoisomerization rate constant ( $k_t$ ) in water. The duration of UV light is set at 0 s, 1 s, 3 s, 7 s, 13 s, 21 s, 31 s, 46 s, 66 s, 100 s, 130 s, and 166 s at 365 nm. Inset: determination of  $k_t$  value of 1 $\subset$ CB[8] upon exposure to UV light at 365 nm.

[8] were investigated by UV/vis spectroscopic experiments. As investigated by UV/vis spectroscopic experiments, both 1 and 1 $\subset$ CB[8] have good light- and thermo-responsive performances. A new absorption band at 321 nm and an isosbestic point at 276 nm were observed after irradiation at 365 nm, which was originated from the photoinduced isomerization of 1 (Supplementary Figures S27). The continuous heating of the solution at  $80^\circ\text{C}$  ultimately resulted in the recovery of original absorption bands, suggesting the regeneration of molecular loop *trans*-1 $\subset$ CB[8]<sup>25</sup>. This optical switching process can be recycled for several times upon alternate exposure to UV irradiation and heating treatment (Supplementary Figures S27, inset). Moreover, employed the first-order kinetics, the *trans*- and *cis*-photoisomerization rate constant ( $k_t$ ) of azobenzene 1 in solution was calculated as  $0.0190 \pm 0.0002 \text{ s}^{-1}$  by plotting the absorbance changes versus time, while this value slightly decreased to  $0.0131 \pm 0.0001 \text{ s}^{-1}$  in the presence of 1.0 equiv of CB[8] (Figure 3, and Supplementary Figures S43 and S44). This result suggests that the association of CB[8] could not significantly affect the photochemical property of azobenzene in 1.

**The controlled interconversion process between the supramolecular complex *trans*-2 $\subset$ CB[8] and [2]pseudorotaxane *cis*-2 $\subset$ CB[8] were investigated by  $^1\text{H}$  NMR titration.** Comparatively, the proton signals of  $\text{H}_{\text{b-e}}$  in the bispyridinium moiety and  $\text{H}_{\text{f,g}}$  adjacent to *trans*-azobenzene moiety in 2 shifted upfield upon complexation with CB[8] (Figure 4b). The axle molecule *trans*-2 was transferred to *cis*-2 with the ratio of 20:80 between *trans*- and *cis*-forms under UV irradiation (Supplementary Figure S40). When the equimolar mixture of *trans*-2 and CB[8] was irradiated under UV light, the characteristic peaks for protons  $\text{H}_{\text{C',D'}}$  on the aliphatic linker shifted to higher field (Figure 4c). These chemical shift changes demonstrate that the photoirradiation could facilitate the movement of CB[8] toward nonaromatic linker to form a [2]pseudorotaxane structure of *cis*-2 $\subset$ CB[8] (Supplementary Figure S35b). Significantly, the loop structure of *trans*-2 $\subset$ CB[8] could be efficiently recovered upon irradiation at 450 nm (Figure 4d).

**The controlled interconversion process between the supramolecular complex of *trans*-2 $\subset$ CB[8] and [2]pseudorotaxane of *cis*-2 $\subset$ CB[8] were further investigated by mass spectrometry.** The peak at  $m/z$  890.9 was assigned to  $\{2\subset\text{CB}[8] - 2\text{Br}\}^{2+}$  (Supplementary Figure S32). The same peak corresponding to the 1:1 inclusion complex of was still observed after irradiation at 365 nm (Supplementary Figure S33). Furthermore, UV/vis spectroscopic results indicate that the reversible switching process of *trans*-2 $\subset$ CB[8] could be reversibly controlled upon exposure to UV and



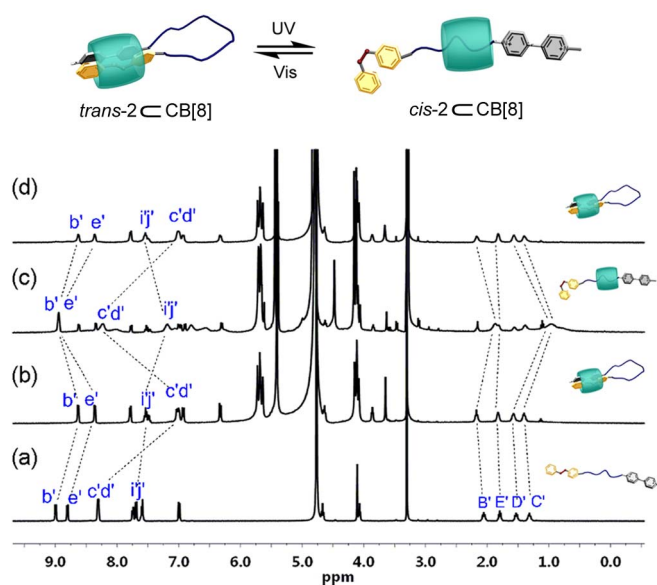


**Figure 4** |  $^1\text{H}$  NMR titration experiments of axle 2 and CB[8] (400 MHz,  $\text{D}_2\text{O}$ ,  $25^\circ\text{C}$ ). (a) *trans*-2; (b) *trans*-2CB[8]; (c) *trans*-2CB[8] after sufficient photoirradiation at 365 nm; (d) the corresponding solution in (c) after sufficient photoirradiation at 450 nm ( $[\text{2}] = [\text{CB}[8]] = 1.0 \text{ mM}$ ).

visible light (Supplementary Figure S42). It should be noted that, although both 1CB[8] and 2CB[8] systems have good photoresponsive property, the absorbance at 351 nm of the photostationary state of 2CB[8] dramatically increased during the period of 70 h, indicating that the inverse transformation from *cis*-2 to *trans*-2 in 2CB[8] system (Supplementary Figure S45). In sharp contrast, since no absorbance change was observed in the same time range, the photostationary state of 1CB[8] could be considered as a stable one in the dark (Supplementary Figure S46). Meanwhile, the photo-stability of naked linear molecule 1 was also investigated by UV/vis spectroscopy. As shown in Figure S50, the absorbance of 1 was continuously changed during a period of 60 h upon UV irradiation. These results clearly demonstrate that CB[8] is an indispensable factor to enhance the photo-stability of 1. The molecular energy minimization was further performed to exhibit two states of supramolecular complex *trans*-2CB[8] and [2]pseudorotaxane *cis*-2CB[8] (Supplementary Figure S35).

**The bistable supramolecular complexes and their corresponding [2]pseudorotaxanes could act as a promising DNA regulator.** Interestingly, it is demonstrated that the supramolecular complexes of *trans*-1CB[8] and *trans*-2CB[8] in this work could exhibit a remarkable DNA condensation ability. The interaction of 1, 2, and their CB[8]-bound complexes with ct-DNA was preliminarily examined by UV/vis spectroscopy<sup>26</sup>. As seen in Figures S52a and S53a, the absorbance of *trans*-1 and *trans*-2 was slightly decreased upon addition of ct-DNA, suggesting that the naked compounds had a weaker interaction with DNA double helix. Comparatively, an obvious hypochromic effect was observed in the presence of CB[8], mainly due to the enhanced binding affinity of ct-DNA with *trans*-1CB[8] and *trans*-2CB[8] (Figures S52b and S53b). Furthermore, the gel retardation assay was performed using *trans*-1CB[8] and *trans*-2CB[8] in the concentration range from 0 to 48  $\mu\text{M}$ . As judged from Figure 5 (Line 0), free pBR322 DNA existed as a mixture of circular supercoiled DNA (form I) and relaxed circular DNA (form II) arising from the single-strand cleavage. Conversely, the amount of supercoiled closed circular pBR322 DNA (form I) was gradually inhibited in the presence of *trans*-1CB[8] and *trans*-2CB[8], and the retardation of DNA was clearly observed in the gel loading wells (Figure 5, Lines 1–7).

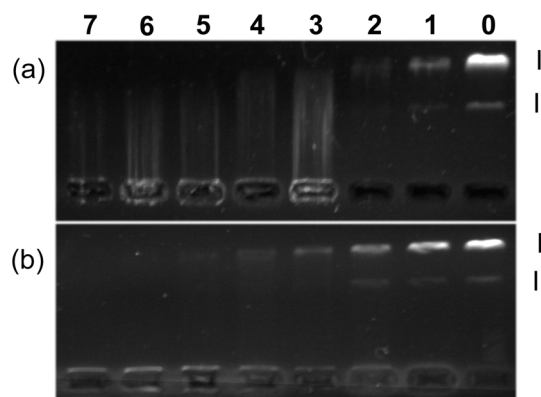


**Figure 5** | Agarose gel electrophoresis assay to investigate the DNA condensation induced by supramolecular complexes. (a) *trans*-1CB[8] and (b) *trans*-2CB[8]; lane 0, DNA alone; lanes 1–7, DNA + complex. The DNA concentration is 5 ng/ $\mu\text{L}$ . The different concentrations of supramolecular complex from lane 1 to lane 7 were 2, 5, 10, 20, 30, 40, 48  $\mu\text{M}$ , respectively.

In addition, as shown in the atomic force microscopic (AFM) images, the free supercoiled pBR322 DNA existed as loose clews on the mica surface (Figure 6a), whereas the originally loose DNA clews turned to the tightly compacted toroids with an average diameter of ca. 130 nm in the presence of supramolecular complex *trans*-2CB[8] (Figure 6b). These results were well consistent with our previous observations<sup>27,28</sup>. Moreover, in the control experiments, *trans*-2CB[8] alone existed as small nanoparticles with an average diameter of ca. 10 nm (Figure S51 in the Supporting Information), mainly due to the formation of amphiphilic aggregation on the mica surface. Consequently, based on these observations, we can deduce that the amphiphilic aggregation could facilitate the communication between CB[8] and nucleotides and then draw the positively charged viologen and DNA backbone much closer, by which the DNA condensation process is achieved with high efficiency.

On the contrary, the [2]pseudorotaxanes of *cis*-1CB[8] or *cis*-2CB[8] showed no condensation ability to pristine DNA, but displayed serious DNA damage upon UV light irradiation (Supplementary Figures S47 and S48). These phenomena could be contributed to the photoinduced electron transfer process, through which the photo-activated viologen moiety in these [2]pseudorotaxanes can generate the reactive oxygen species to destroy the DNA structures<sup>26,29</sup>. Comparatively, no DNA damage was observed with the supramolecular complexes of *trans*-1CB[8] and *trans*-2CB[8] in the dark or by irradiating pBR322 DNA alone in the control experiments (Supplementary Figure S49), indicating that the DNA damage was attributed to the reduced viologen in *cis*-1CB[8]

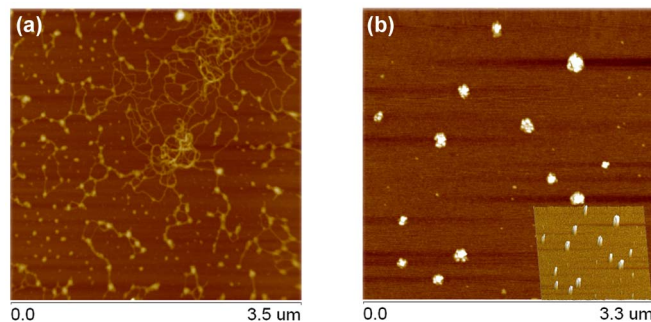


**Figure 6** | AFM images showing the condensation effect of the resultant complex. (a) free pBR322 DNA (1 ng/ $\mu\text{L}$ ), (b) DNA condensation induced by *trans*-2CB[8] (50 ng/ $\mu\text{L}$ ).



and *cis*-2CCB[8]. Structurally, the viologen moiety in the ‘unlocked’ conformer of *cis*-1CCB[8] is exposed to aqueous solution, which subsequently leads to the DNA damage. However, in the case of *trans*-1CCB[8], the captivity of viologen moiety by CB[8] greatly prevents DNA from being damaged, and thus the DNA condensation becomes preferred. As seen in Figure S54, no cleavage was observed in 2CCB[8] without light irradiation, indicating that the process of DNA photocleavage is triggered by external light stimulus. Furthermore, KI and DMSO were added as scavengers to study the mechanism of DNA photocleavage. It is found that the cleavage was seriously inhibited in the presence of singlet oxygen ( $^1\text{O}_2$ ) scavenger KI or hydroxyl radical ( $\cdot\text{OH}$ ) scavenger DMSO, revealing that  $^1\text{O}_2$  and  $\cdot\text{OH}$  were the reactive species responsible for the DNA cleavage reaction.

## Discussion

Combined with the spectroscopic and microscopic results mentioned above, the molecular binding behaviors between CB[8] and positively charged azobenzene in our case have the following common features: (a) Different from the reported results that the radical cation dimers and the pseudorotaxane of bispyridinium salts can be transformed upon addition of CB[8], it is found that upon light irradiation, the existence of positive charges onto azophenyl backbone can greatly prevent CB[8] from interacting with bispyridinium moieties and thus make CB[8] standing at the azophenyl terminals; (b) Compared to the control compounds without imidazolium group, the multiply charged axle component could greatly increase the stability of supramolecular complex, ultimately leading to the bistable ‘locked’ and ‘unlocked’ states in our synergic system; (c) Importantly, considering the different binding states of bispyridinium unit, the objective of this present study is to describe the biological functionality of supramolecular machines, that is, these supramolecular complexes and their corresponding [2]pseudorotaxanes have different DNA condensation and damage abilities toward light stimulus, accompanied by a remarkable morphology change of DNA molecules.

In conclusion, taking advantage of the noncovalent interactions of CB[8] toward *trans*- and *cis*- isomers of positively charged azobenzene, we have demonstrated two types of supramolecular complexes, in which the interconversion of ‘locked’ and ‘unlocked’ states could be efficiently modulated in a reversible manner by adopting a stimuli-responsive guest capture and release strategy. The obtained supramolecular complexes and their corresponding [2]pseudorotaxanes could also act as the promising DNA concentrators and cleavage agents, as exemplified by the good binding abilities toward supercoiled pBR322 DNA. We also envision that these host–guest systems between CB[8] and positively charged azobenzene not only endows these supramolecular complexes with fascinating photochemical activity, but also provides a novel operating principle that can mimic the cooperative and multipoint binding modes in biological systems.

## Methods

**Instrumentation and methods.** All chemicals were commercially available unless noted otherwise. 1-(4-(Bromomethyl)phenyl)-2-phenyldiazene (4)<sup>20</sup>, 1-(6-bromohexyl)-1'-methyl-4,4'-bipyridine-1,1'-dium (6)<sup>30</sup>, (*E*)-1-(4-(6-bromohexyloxy)phenyl)-2-phenyldiazene (7)<sup>31</sup> 1-methyl-4-(pyridin-4-yl)pyridinium (8)<sup>32</sup> were prepared according to the literatures procedures. NMR data were recorded on 300 M, 400 M and 600 M spectrometers, respectively, and chemical shifts were recorded in parts per million (ppm). All chemical shifts were referenced to the internal MeOH signal at 3.34 ppm<sup>33</sup>. UV/vis spectra were recorded in a conventional quartz cell (light path = 10 mm) and a UV spectrophotometer equipped with a temperature controller to keep the temperature at 25°C. Mass spectra were performed on an ESI mode MS.

**Atomic force microscopic (AFM).** For AFM measurements, a drop of sample suspension was dropped onto newly clipped mica and then air-dried, then examined by using an atomic force microscope (Veeco Company, Multimode, Nano IIIa) in tapping mode in air under ambient conditions.

**Isothermal titration microcalorimetry.** The ITC instrument was calibrated chemically by measurement of the complexation reaction of  $\beta$ -cyclodextrin with cyclohexanol and the obtained thermodynamic data were shown to be in good agreement (error < 2%) with the literature data. All microcalorimetric titrations between  $\text{MV}^{2+}\cdot\text{CB}[8]$  and *trans*-3 guest were performed in aqueous phosphate buffer solution (pH 7.2) at atmospheric pressure and 25.00°C. Each solution was degassed and thermostated before titration experiment.

**Preparation of the sample for agarose gel electrophoresis analysis.** In our experiment, ct-DNA was used in UV/vis spectroscopy experiments, and plasmid DNA pBR322 was used as the model DNA for agarose gel electrophoresis analysis. A mixture of DNA (0.2  $\mu\text{g } \mu\text{L}^{-1}$ ) and aqueous samples in 1 mM EDTA/10 mM Tris buffer (pH 8.0) was incubated at room temperature. All solutions were stored at 4°C before use.

- Wang, J. & Feringa, B. L. Dynamic Control of Chiral Space in a Catalytic Asymmetric Reaction Using a Molecular Motor. *Science* **331**, 1429–1432 (2011).
- Harada, A., Hashidzume, A., Yamaguchi, H. & Takashima, Y. Polymeric Rotaxanes. *Chem. Rev.* **109**, 5974–6023 (2009).
- Kay, E. R., Leigh, D. A. & Zerbetto, F. Synthetic Molecular Motors and Mechanical Machines. *Angew. Chem., Int. Ed.* **46**, 72–191 (2007).
- Ma, X. & Tian, H. Bright functional rotaxanes. *Chem. Soc. Rev.* **39**, 70–80 (2010).
- Kelly, T. R. *et al.* A Molecular Brake. *J. Am. Chem. Soc.* **116**, 3657–3658 (1994).
- Khuong, T. A. V. *et al.* Rotational Dynamics in a Crystalline Molecular Gyroscope by Variable-Temperature  $^{13}\text{C}$  NMR,  $^1\text{H}$  NMR, X-Ray Diffraction, and Force Field Calculations. *J. Am. Chem. Soc.* **129**, 839–845 (2007).
- Badjić, J. D. *et al.* A Molecular Elevator. *Science* **303**, 1845–1849 (2004).
- Muraoka, T., Kinbara, K., Kobayashi, Y. & Aida, T. Light-Driven Open-Close Motion of Chiral Molecular Scissors. *J. Am. Chem. Soc.* **125**, 5612–5613 (2003).
- Cheng, H.-B., Zhang, H.-Y. & Liu, Y. Dual-Stimulus Luminescent Lanthanide Molecular Switch Based on an Unsymmetrical Diarylperfluorocyclopentene. *J. Am. Chem. Soc.* **135**, 10190–10193 (2013).
- Jeon, W. S. *et al.* A [2]Pseudorotaxane-Based Molecular Machine: Reversible Formation of a Molecular Loop Driven by Electrochemical and Photochemical Stimuli. *Angew. Chem., Int. Ed.* **42**, 4097–4100 (2003).
- Jeon, W. S. *et al.* Molecular Loop Lock: A Redox-Driven Molecular Machine Based on a Host-Stabilized Charge-Transfer Complex. *Angew. Chem. Int. Ed.* **44**, 87–91 (2005).
- Tian, F., Jiao, D., Biedermann, F. & Scherman, O. A. Orthogonal switching of a single supramolecular complex. *Nat. Commun.* **3**, 1207–1215 (2012).
- del Barrio, J. *et al.* Photocontrol over Cucurbit[8]uril Complexes: Stoichiometry and Supramolecular Polymers. *J. Am. Chem. Soc.* **135**, 11760–11763 (2013).
- Hubbell, J. A. Enhancing Drug Function. *Science* **300**, 595–596 (2003).
- Hamley, I. W. & Castelletto, V. Biological Soft Materials. *Angew. Chem., Int. Ed.* **46**, 4442–4455 (2007).
- Schuster, G. B. Long-Range Charge Transfer in DNA: Transient Structural Distortions Control the Distance Dependence. *Acc. Chem. Res.* **33**, 253–260 (2000).
- Liu, Y. *et al.* Reversible 2D Pseudopolyrotaxanes Based On Cyclodextrins and Cucurbit[6]uril. *J. Org. Chem.* **72**, 280–283 (2007).
- Ke, C.-F. *et al.* Controllable DNA condensation through cucurbit[6]uril in 2D pseudopolyrotaxanes. *Chem. Commun.* 3374–3376 (2007).
- Hwang, I. *et al.* Cucurbit[7]uril: A Simple Macrocyclic, pH-Triggered Hydrogelator Exhibiting Guest-Induced Stimuli-Responsive Behavior. *Angew. Chem., Int. Ed.* **46**, 210–213 (2007).
- Yu, G. *et al.* Pillar[6]arene-Based Photoresponsive Host–Guest Complexation. *J. Am. Chem. Soc.* **134**, 8711–8717 (2012).
- Dube, H., Ams, M. R. & Rebek Jr, J. Supramolecular Control of Fluorescence through Reversible Encapsulation. *J. Am. Chem. Soc.* **132**, 9984–9985 (2010).
- Lee, J. W. *et al.* Unprecedented host-induced intramolecular charge-transfer complex formation. *Chem. Commun.* 2692–2693 (2002).
- Guo, J. B., Jiang, Y. & Chen, C. F. Self-Assembled Interwoven Cages from Triptycene-Derived Bis-Macrotricyclic Polyether and Multiple Branched Paraquat-Derived Subunits. *Org. Lett.* **12**, 5764–5767 (2010).
- Tomimasu, N. *et al.* Social Self-Sorting: Alternating Supramolecular Oligomer Consisting of Isomers. *J. Am. Chem. Soc.* **131**, 12339–12343 (2009).
- Dube, H., Ajami, D. & Rebek Jr, J. Photochemical Control of Reversible Encapsulation. *Angew. Chem. Int. Ed.* **49**, 3192–3195 (2010).
- Zhang, T. *et al.* Interaction of DNA and a series of aromatic donor–viologen acceptor molecules with and without the presence of CB[8]. *Phys. Chem. Chem. Phys.* **13**, 9789–9795 (2011).
- Liu, Y. *et al.* Construction and DNA Condensation of Cyclodextrin-Based Polypseudorotaxanes with Anthryl Grafts. *J. Am. Chem. Soc.* **129**, 10656–10657 (2007).
- Liu, Y. *et al.* A Luminescent  $\beta$ -Cyclodextrin-Based Ru(phen)<sub>3</sub> Complex as DNA Compactor, Enzyme Inhibitor, and Translocation Tracer. *ACS Nano* **1**, 313–318 (2007).
- Hariharan, M. *et al.* Photoinduced DNA damage efficiency and cytotoxicity of novel viologen linked pyrene conjugates. *Chem. Commun.* **46**, 2064–2066 (2010).



30. Bonchio, M. *et al.* Thermal behaviour and electrochemical properties of bis(trifluoromethanesulfonyl)amide and dodecatungstosilicate viologen dimers. *Phys. Chem. Chem. Phys.* **14**, 2710–2717 (2012).
31. Mannsfeld, S. C. B. *et al.* The Structure of [4-(Phenylazo)phenoxy]hexane-1-thiol Self-Assembled Monolayers on Au(111). *J. Phys. Chem. B* **106**, 2255–2260 (2002).
32. Oh, K. J., Kevin, J., Hugenberg, V. & Plaxco, K. W. Peptide Beacons: A New Design for Polypeptide-Based Optical Biosensors. *Bioconjugate Chem.* **18**, 607–609 (2007).
33. Gottlieb, H. E., Kotlyar, V. & Nudelman, A. NMR Chemical Shifts of Common Laboratory Solvents as Trace Impurities. *J. Org. Chem.* **62**, 7512–7515 (1997).

## Acknowledgments

We thank 973 Program (2011CB932502) and NNSFC (Nos. 20932004, 91227107, and 21102075) for financial support.

## Author contributions

Y.L. conceived the project and designed this supramolecular system. H.B.C. and C.X. contributed to the synthesis work and analyzed the data and co-wrote the paper with Y.M.Z. All authors discussed the results and commented on the manuscript, and reviewed this manuscript.

## Additional information

**Supplementary information** accompanies this paper at <http://www.nature.com/scientificreports>

**Competing financial interests:** The authors declare no competing financial interests.

**How to cite this article:** Cheng, H.-B., Zhang, Y.-M., Xu, C. & Liu, Y. Photoresponsive Supramolecular Complexes as Efficient DNA Regulator. *Sci. Rep.* **4**, 4210; DOI:10.1038/srep04210 (2014).



This work is licensed under a Creative Commons Attribution-NonCommercial-ShareAlike 3.0 Unported license. To view a copy of this license, visit <http://creativecommons.org/licenses/by-nc-sa/3.0>